



**AIAA 2002-4809**

**Aerodynamics of Mars Odyssey**

Naruhisa Takashima

AMA Inc.  
Hampton, VA

Richard G. Wilmoth

NASA Langley Research Center  
Hampton, VA

**AIAA Atmospheric Flight Mechanics  
Conference & Exhibit  
5-8 August, 2002  
Monterey, California**

## Aerodynamics of Mars Odyssey

Naruhisa Takashima\*  
AMA Inc.  
Hampton, VA

Richard G. Wilmoth<sup>†</sup>  
NASA Langley Research Center  
Hampton, VA

### ABSTRACT

Direct Simulation Monte Carlo and free-molecular analyses were used to provide aerothermodynamic characteristics of the Mars Odyssey spacecraft. The results of these analyses were used to develop an aerodynamic database that was used extensively for the pre-flight planning and in-flight execution for the aerobraking phase of the Mars Odyssey mission. During aerobraking operations, the database was used to reconstruct atmospheric density profiles during each pass. The reconstructed data was used to update the atmospheric model, which was used to determine the strategy for subsequent aerobraking maneuvers. The aerodynamic database was also used together with data obtained from on-board accelerometers to reconstruct the spacecraft attitudes throughout each aerobraking pass. The reconstructed spacecraft attitudes are in good agreement with those determined by independent on-board inertial measurements for all aerobraking passes. The differences in the pitch attitudes are significantly less than the preflight uncertainties of  $\pm 2.9\%$ . The differences in the yaw attitudes are influenced by zonal winds. When latitudinal gradients of density are small, the differences in the yaw attitudes are significantly less than the preflight uncertainties.

### Introduction

On January 11, 2002, NASA's Mars Odyssey spacecraft successfully completed its aerobraking phase of the mission. Launched on April 7, 2001 aboard Boeing's Delta II 7925, Mars Odyssey arrived at Mars on October 24, 2000. A Mars Orbit Insertion (MOI) burn placed the spacecraft in a highly elliptical capture orbit. After completing the "walk in" phase of aerobraking, where the periapsis altitude was reduced to approximately 130 km, the "main phase" of aerobraking was commenced. The period of the orbit was gradually reduced from the initial orbit period of 18 hours to approximately 2 hours. The main phase of aerobraking lasted 75 days with 336 aerobraking passes. The "walk out" phase was initiated on January 11, 2002, and the spacecraft was placed in its final 400 km circular science orbit.

Aerobraking utilizes the atmospheric drag to make gradual changes in the orbit. By successfully completing the aerobraking phase of the mission, Mars Odyssey became the second successful planetary

mission designed specifically to utilize aerobraking as a primary means of achieving its mission objectives. Using the aerobraking technique saved approximately 200 kg of propellant mass for Mars Odyssey. Prior to the Mars Odyssey mission, aerobraking was successfully used in two missions. The first application of aerobraking in a planetary mission was during the Magellan mission at Venus where the eccentricity of the orbit was reduced from 0.39 to 0.03 in about 70 days.<sup>1</sup> The second application of aerobraking was for the Mars Global Surveyor (MGS) mission. For the MGS mission, aerobraking was an enabling technology, where the reduction in the propulsive capability afforded by the use of aerobraking was needed to satisfy the payload capabilities of the Delta II launch vehicle, during a November 1996 Earth-to-Mars launch opportunity. A total of approximately 900 aerobraking orbits, which decreased the orbit period by approximately 43 hours, were accomplished in two phases during its mission.<sup>2</sup>

Like the two predecessors, the primary drag surfaces of Mars Odyssey are its solar arrays and the pace of aerobraking is dictated by the solar array heating. For the Mars Odyssey mission, the rate at which the period of the orbit is reduced by aerobraking was dictated by achieving desirable local true solar time (LTST) at the end of aerobraking while keeping the temperature of the solar arrays below that of the flight allowable solar array temperature of 175° C. This was accomplished by keeping the periapsis of the orbit within a specified freestream heating rate corridor during aerobraking.

\* Senior Project Engineer, Member, AIAA.

<sup>†</sup> Aerospace Engineer, Aerothermodynamics Branch, Senior Member, AIAA.

Based on MGS aerobraking experience, 80%  $2\sigma$  orbit-to-orbit natural atmospheric density variation was allocated for the mission. Applying additional safety margins to those numbers, the top of the corridor was defined as providing 100% margin to the flight allowable freestream heating rate. The bottom of the corridor was defined by subtracting the width of the corridor, which was set at  $0.18 \text{ W/cm}^2$ , from top of the corridor. The spacecraft was kept within the corridor by monitoring the atmospheric densities and performing periodic aerobraking propulsive maneuvers (ABM).<sup>3</sup>

All of the aerobraking took place at altitudes where the densities are sufficiently low that the flow is in the rarefied transitional regime. To accurately predict the aerodynamic characteristic of the spacecraft in the rarefied transitional flow regime, Direct Simulation Monte Carlo (DSMC) and free molecular techniques were used. The results from the calculations were used to create the aerodynamic database of the spacecraft that was used extensively in both pre-flight predictions and in-flight analyses, and played a key role in success of the aerobraking phase of the mission.

### DSMC Calculation

#### Computational Method

The DSMC calculations were performed using DDAC, which is the parallel implementation of the program DAC (DSMC Analysis Code).<sup>4,5</sup> In DAC, the gas collisions are modeled using the variable-hard-sphere (VHS) model developed by Bird<sup>6</sup>, and the Larsen-Borgnakke model is used for internal energy exchanges. The geometry surface is represented by unstructured triangular elements that are embedded in a two-level Cartesian grid for the flow field calculation. The solution from the first level of grid cells, which are uniform in size, is used for grid refinement to create the second-level cells. The grid is refined based on local conditions, thus allowing the program to meet the spatial resolution requirements without excessive global refinement. The grid cells are typically refined such that on average the second-level cells have dimensions less than the local mean free path. The local simulation parameters are set such that there are nominally 10 simulated molecules in each cell, and the local time step is typically dictated by the local flow time for the problems considered.

For all calculations the wall collisions were assumed to be fully diffuse, i.e., an accommodation coefficient of one was specified, with spacecraft wall temperature of constant 300 K. The composition of Mars atmosphere was assumed to be 95.37%  $\text{CO}_2$  and 4.63%  $\text{N}_2$  by mole with a freestream temperature of 144.7 K and velocity of 4811 m/s. A reference temperature of 300 K and a viscosity-temperature-index of 0.71 were

used for the VHS model. The computational geometry shown in Figure 1 was provided by Lockheed Martin Astronautics (LMA) and represents the best pre-flight estimate of the nominal aerobraking configuration.

Free molecular and continuum results were obtained using DACfree.<sup>7</sup> DACfree is a companion code to DAC, which utilizes the same unstructured triangular surface mesh. The free molecular forces, moments and heat transfer are calculated with analytical free-molecular analysis and line-of-sight shadowing, and a modified Newtonian method is used to calculate the continuum forces and moments on the geometry. The continuum results are used mainly to guide the development of curve fitting or bridging-function techniques for the aerodynamic coefficients since Odyssey aerobraking always took place at Knudsen numbers well above those for continuum flow.

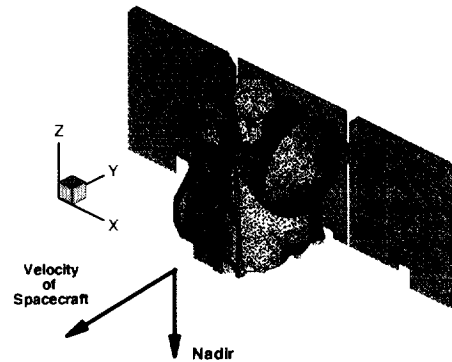


**Figure 1. Computational Geometry Model.**

#### DSMC Results

Figure 2 shows the non-dimensionalized density contour plots in a plane approximately 1 m above the bottom of the spacecraft for freestream densities of  $10 \text{ kg/km}^3$  and  $100 \text{ kg/km}^3$ , where the latter value represents the highest density expected to be encountered during aerobraking. The plots show the typical diffuse shock layers that occur in rarefied transitional flow, with the layer getting pressed to the surface as the freestream density increases. Figure 3 shows the surface pressure contours for a freestream density of  $100 \text{ kg/km}^3$  at the nominal attitude. The plot shows that the spacecraft bus shields the center solar array and the edges of outboard solar arrays from the on-coming flow.

The total number of molecules in the simulations performed varied from 0.5 million for  $0.1 \text{ kg/km}^3$  runs to 2.5 million for  $100 \text{ kg/km}^3$  runs. Most cases were run for over 10,000 time steps to ensure adequate sample size.

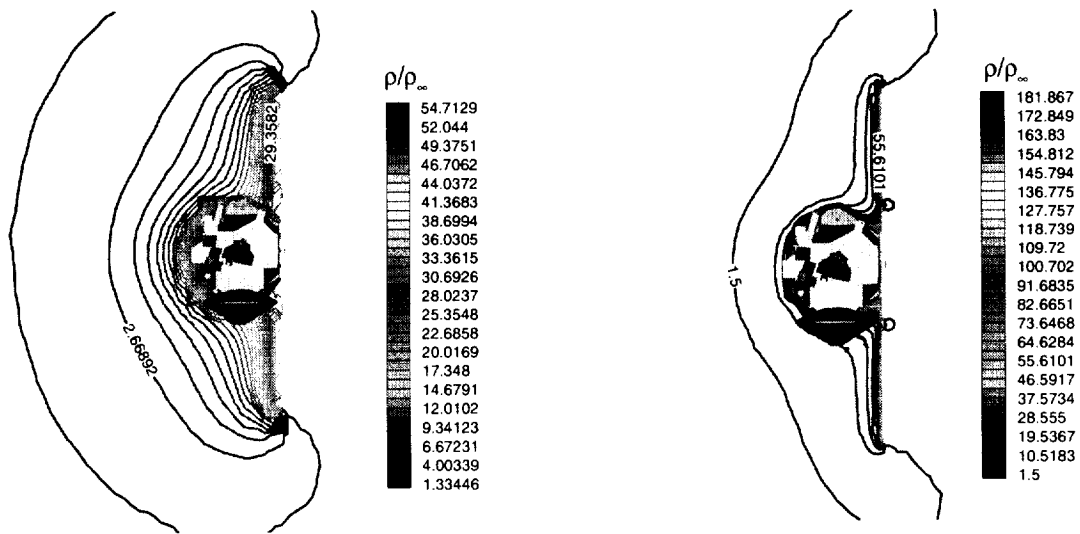


Figure 2. Nondimensional density contour plots.

measurements of the inertial attitude of the spacecraft and the trajectory determined from other navigational data.

#### Database Construction

The aerodynamic database of Mars Odyssey was constructed by combining results from free molecular/continuum analysis computed with DACfree and DSMC results computed with DDAC. Free-molecular analyses were used to provide variations of aerodynamic coefficients vs. spacecraft attitude (pitch and yaw), and DSMC calculations performed over a limited range of attitudes and atmospheric densities were used to account for variations in coefficients with freestream density. Once the solutions were obtained, multivariate curve fits were performed to construct an “enriched” database of aerodynamic coefficients with sufficient resolution for use in both 3DOF and 6DOF trajectory simulations. These curve fits covered a pitch and yaw attitude range of  $\pm 60^\circ$  and density range of  $10^{-4}$  to  $2500 \text{ kg/km}^3$  where the lower value represents the free molecular limit and the higher value represents the continuum limit.

The aerodynamic computational matrix was defined based on rotation angles in the spacecraft body coordinate systems, where pitch ( $\theta$ ) is defined as the first rotation about the X-axis and yaw ( $\phi$ ) is defined at the second rotation about the Z-axis. Free molecular calculations were performed for yaw and pitch angles of  $-60^\circ$  to  $+60^\circ$  in 5-degree increments. DSMC calculations were performed for densities of 0.1, 1.0, 3.162, 10.0, 31.62 and  $100 \text{ kg/km}^3$  at pitch and yaw

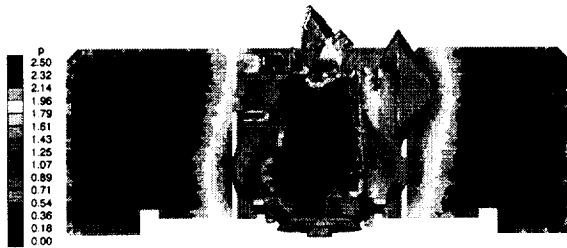


Figure 3. Surface pressure contours for freestream density of  $100 \text{ kg/km}^3$  at the nominal attitude.

#### Aerodynamic Database

The objective of the rarefied flow analyses was to develop an aerodynamic database for Mars Odyssey. The database was used to extract atmospheric densities from flight data and was incorporated into the Jet Propulsion Laboratory’s (JPL) trajectory code, which was used to devise strategies for ABM on a daily basis.<sup>3</sup> It was also used by the NASA Langley Flight Mechanics Team to perform three-degree-of-freedom (3DOF) and six-degree-of-freedom (6DOF) trajectory simulations.<sup>8</sup> Lastly, the aerodynamic force coefficients from the database were used together with the three-component accelerometer data to determine the relative wind attitude of the spacecraft. This attitude was then compared with that obtained from independent

angles of  $-60^\circ$ ,  $0^\circ$  and  $+60^\circ$ , resulting in total of 54 DSMC calculations.

The database was enriched by assuming that the shape of each coefficient curve for a given angle sweep at any density is the same as the free molecular result and that values of each aerodynamic coefficient approach free molecular values as the density decreases and Newtonian values (which are also calculated by DACfree) as the density increases. For a given density, the free molecular coefficient curve in pitch was scaled using the DSMC results, and the curve was offset to match the coefficient value at  $\phi = 0^\circ$  for each pitch angles as shown in Figure 4. By repeating the procedure, but exchanging the direction and performing the scaling and offset for every  $5^\circ$  in yaw angle, the variations of force and moment coefficients with attitude are determined. Figure 5 shows the contour plots of the force coefficients for a freestream density of  $10 \text{ kg/km}^3$ , and Figure 6 shows the variation of axial force coefficient with freestream density for the nominal attitude of yaw and pitch angles of 0 degree. The line in the density variation plot is formed with the values returned from the interpolation routine that accompanies the aerodynamic database.

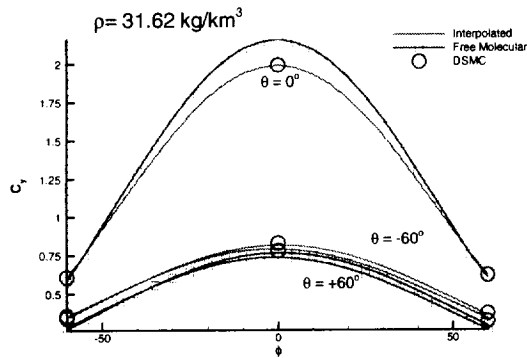


Figure 4. Aerodynamic database enrichment.

#### Database Uncertainty

The knowledge of the accuracy of the aerodynamic database and the accompanying interpolation routines are important for determining the atmospheric density and planning of the aerobraking maneuvers. Hence, prior to the aerobraking of the mission, the database and the accompanying routines were verified and validated to the extent which was possible. Table 1 summarizes the uncertainty associated with the aerodynamic database. The uncertainties of the database for the force coefficients were estimated to be  $\pm 2.9\%$  and are included in Figure 6. The sources of uncertainty include computational errors, physical model errors and boundary condition errors as listed in

Table 1. Errors were estimated from parametric sensitivity studies when direct data was not available. The largest error source was the uncertainty in the accommodation coefficients. The symbols in the figure represent all the DSMC runs that were made to establish the uncertainty due to computational errors. The interpolation errors of the database were determined as less than 0.1% by reproducing known dataset.

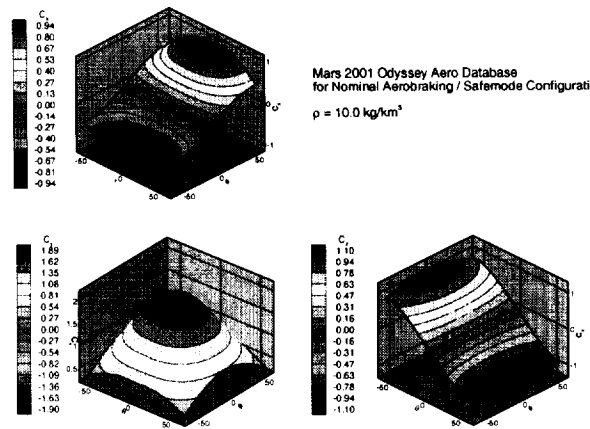


Figure 5. Variation of axial force coefficient at the nominal attitude with free stream density.

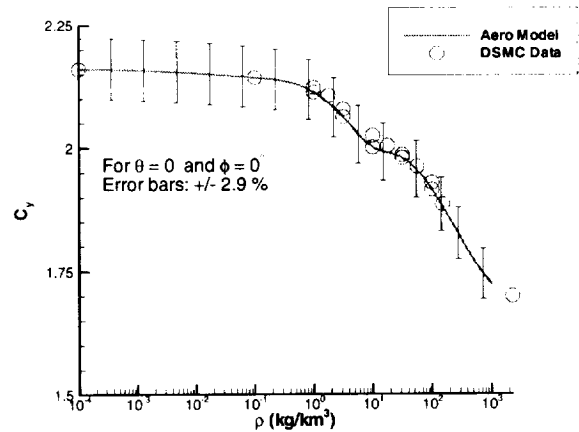


Figure 6. Variation of axial force coefficient with density at the nominal attitude.

To monitor the accuracy of the aerodynamics database, measured spacecraft attitude during aerobraking passes was compared to the spacecraft attitude extracted from the database using measured acceleration ratios. Uncertainties in the aerodynamic database translate directly into uncertainties in the relative wind attitude (pitch and yaw) that can be deduced from the accelerometer measurements. Figure 7 shows the variation of error in the acceleration ratio

$\delta A_x/A_y$ , with density as functions of acceleration data uncertainty and the database uncertainty. These uncertainties must be combined with those of the accelerometers, which were estimated to be a constant  $0.54 \text{ mm/s}^2$  by Jim Chapel of LMA. The estimated uncertainties given in Table 1 are for the coefficients that are nondimensionalized by density (through the dynamic pressure) and therefore, the error in acceleration ratio associated with the database are independent of density. However, the accelerometer error is assumed to be a constant dimensional value, and since the axial acceleration,  $A_y$ , is proportional to density, the error in the ratio decrease in inverse proportion to density. The result of this behavior is that attitude uncertainties are dominated by accelerometer errors at low densities and by aerodynamic database errors at high densities.

Figure 8 shows the sensitivity of pitch angle determination with respect to the error in acceleration ratio. The figure shows that for  $\phi = 0 \text{ deg.}$  and  $\theta = -20 \text{ deg.}$ , the error in pitch angle varies linearly with the error in acceleration ratio but it does not vary with density for a given acceleration error. For the density range encountered during aerobraking, the results from Figure 7 and Figure 8 show that the pitch angle error should be less than 2.0 degrees and well within the flight controller deadband of  $\pm 20^\circ$  for a wide range of densities. The results shown are for the pitch angle but the sensitivity of the yaw angle is similar.

#### Flight Data

Figure 9 shows the atmospheric density during aerobraking pass 183. The atmospheric density,  $\rho$  is reconstructed using the equation,

$$a_y = \frac{\rho V^2 C_y S}{2m} \quad (1)$$

where  $a_y$  is the axial-acceleration,  $m$  is the mass,  $V$  is the velocity,  $C_y$  is the axial force coefficient and  $S$  is the reference area of the spacecraft. Since the axial-force coefficient is a function of both spacecraft attitude and freestream density, an iterative process is required to determine the density. The attitude of the spacecraft is determined from the inertial measurement unit (IMU) data and the spacecraft velocity, which is calculated along an aerobraking trajectory from the periapsis state with J2 gravitational term and assuming a rigid rotating atmosphere. The axial acceleration is measured by the accelerometer on the spacecraft. The correct density is determined once the product of density, axial force coefficient and known values equal the measured axial-acceleration. Details concerning density determination

and atmospheric modeling for the Mars Odyssey mission can be found in Ref. 9.

Since the accuracy of the atmospheric density data is directly linked to the accuracy of the aerodynamic database, the performance of the aerodynamic database was monitored during the entire aerobraking phase of the mission by comparing the "measured" spacecraft attitude with reconstructed data using accelerometer ratios and the aerodynamic database. The ratios of accelerometer measurements,  $A_x/A_y$  and  $A_z/A_y$ , are equivalent to the ratios of force coefficients  $C_x/C_y$  and  $C_z/C_y$ , can be used to extract the spacecraft attitude from the database. Figure 10 shows spacecraft attitude comparison for aerobraking pass 183. Good agreement between the two sets of data, well within the uncertainties, which are now a combination of the database uncertainty and the accelerometer uncertainty, are observed through the entire aerobraking pass. This pass was atypical in that there was very little atmospheric variability during this pass. Atmospheric analysis showed that there was very little latitudinal variation in density for this particular pass. A more typical pass is represented in Figure 11. The figure shows the spacecraft attitude comparison for aerobraking pass 170. The pitch attitude comparison shows that results derived from the aerodynamic database match the data from flight measurements, similar to pass 183. However, there is a distinct off set between the two curves near the periapsis for the yaw attitude comparison, which suggests presence of zonal winds.

The presence of zonal winds is illustrated in Figure 12. The figure shows the spacecraft attitude comparisons for aerobraking passes 112 and 165. For both passes, the periapsis latitude and longitude are approximately  $80^\circ$  North and  $75^\circ$  East. Good agreement in pitch attitude is observed for pass 165 but not for pass 112. This discrepancy in the pitch attitude appeared to be a consistent bias speculated to be caused by a small error in the computational geometry model and was later corrected after P120. However, the differences in yaw angle were consistent with the possible existence of a strong westerly zonal wind. As mentioned previously, the attitude of the spacecraft is based on the spacecraft velocity defined by the Accelerometer team of Mars Odyssey Operation Team. The velocity of the spacecraft along an aerobraking trajectory is calculated from the periapsis state with J2 gravitational term and assuming rigid rotating atmosphere; hence, any wind with sufficient magnitude will cause differences in attitude based on IMU data and attitude derived from the aerodynamic model with accelerometer data. The yaw angle differences for the two passes show the possible existence of strong westerly zonal winds. Although the latitude and longitude of the periapsis of the two orbits are similar,

the latitude of the trajectory is increasing for P112, whereas the latitude of the trajectory is decreasing for P165, therefore, the westerly wind causes opposite shifts in yaw attitude as shown by these comparisons.

**Summary**

The majority of passes showed large atmospheric variability and the existence of zonal winds. Overall, comparisons from all aerobraking passes show that the aerodynamic database and the model reconstruct the flight data with the expected accuracy. Figure 13 and Figure 14 show the mean and the RMS of the differences in spacecraft attitude for each aerobraking pass. The step reduction in pitch attitude difference is caused by the pitch model modification that was applied to the analysis based on flight data collected from the first 120 passes to correct for the consistent

bias referred to earlier. After the introduction of the new pitch model, the differences in pitch attitude became significantly less than the preflight uncertainty. The mean of the differences and the RMS of the differences for passes after 120 are approximately zero and  $-1.0$  deg., respectively.

Corrections to the yaw predictions were never introduced since there was too much scatter in the differences in the yaw attitude comparisons to allow an accurate correlation with any credible zonal wind model. However, Figure 13 shows a strong qualitative indication that such winds are present. The figure shows that the mean differences are initially negative but as the trajectory changes from north bound to south bound the differences become positive, which can be explained by the presence of zonal winds. For most of the aerobraking passes the RMS of the differences in yaw attitude were less than 2.5 deg.

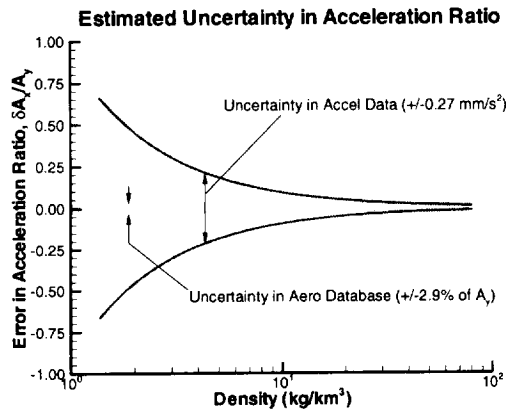


**Figure 7. Variation of uncertainty in acceleration ratio.**

**Sensitivity of Pitch Angle to Acceleration Ratio Error**

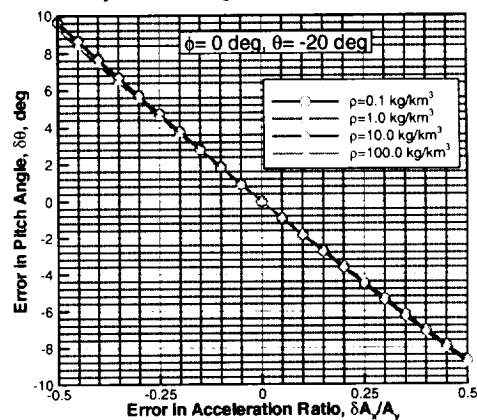


**Figure 8. Sensitivity of pitch angle to acceleration ratio error.**

**Table 1. Force Coefficient Uncertainty**

Source of Uncertainty	Relative	Minimum	Source of Error Estimate
<b>Computational Errors</b>			
Statistical Sampling	$\pm 0.05\%$	$\pm 0.001$	Computational Sample Size
Grid	$\pm 1.0\%$	$\pm 0.0$	Grid Sensitivity Studies
<b>Physical Model Errors</b>			
Gas Collision Models	$\pm 1.0\%$	$\pm 0.0$	Cross-Section Data
Accommodation Coefficient	$\pm 2.5\%$	$\pm 0.03$	Flight/Laboratory Data
<b>Boundary Condition</b>			
Atmosphere Temperature	$\pm 0.1\%$	$\pm 0.0$	CBE
Surface Temperature	$\pm 0.5\%$	$\pm 0.0$	Thermal Model
Geometry	Not Known		
<b>Total RMS Uncertainty</b>	<b><math>\pm 2.9\%</math></b>	<b><math>\pm 0.03\%</math></b>	

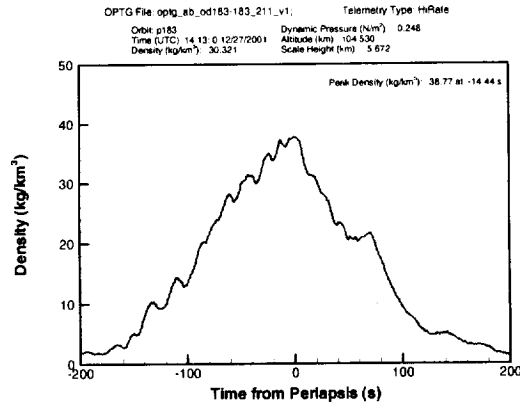


Figure 9. Density during aerobraking pass 183.

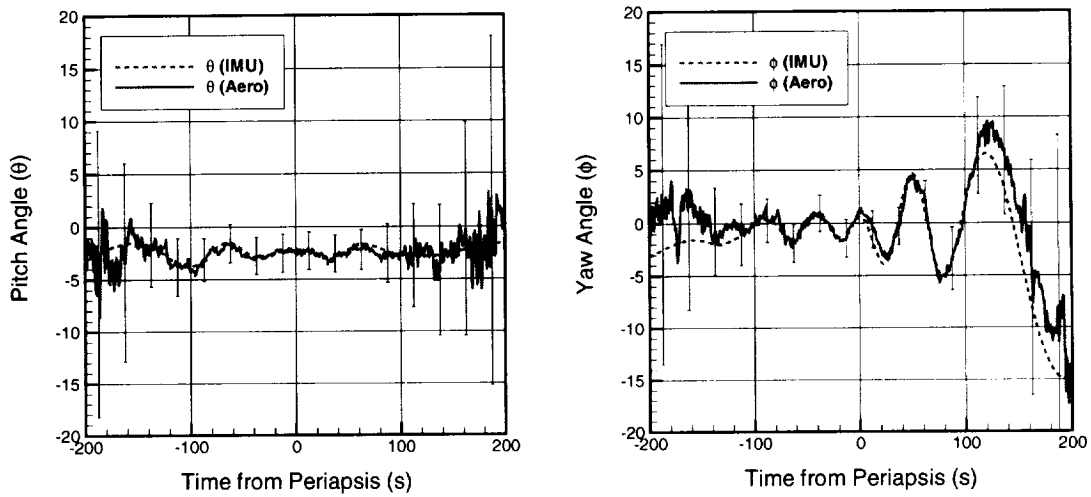


Figure 10. Spacecraft attitude comparison for aerobraking pass 183.

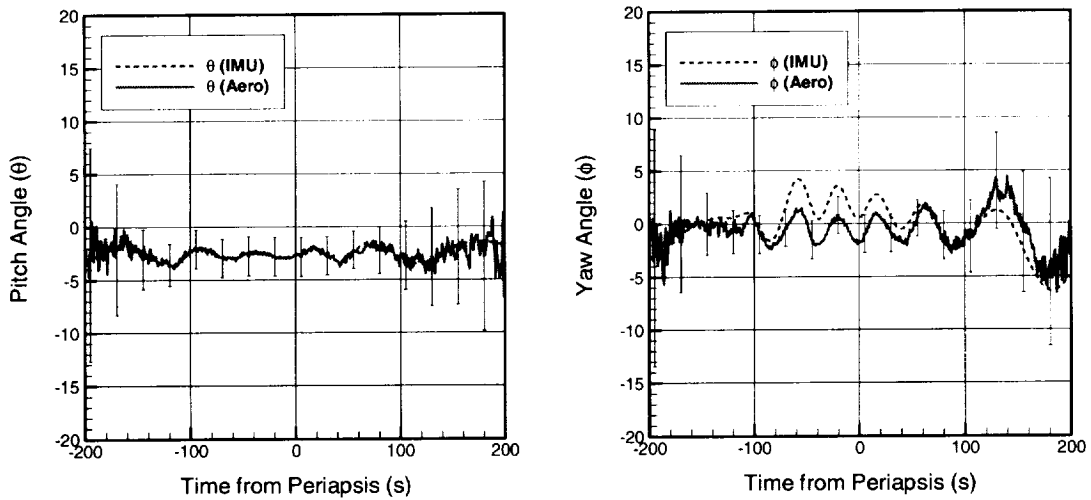
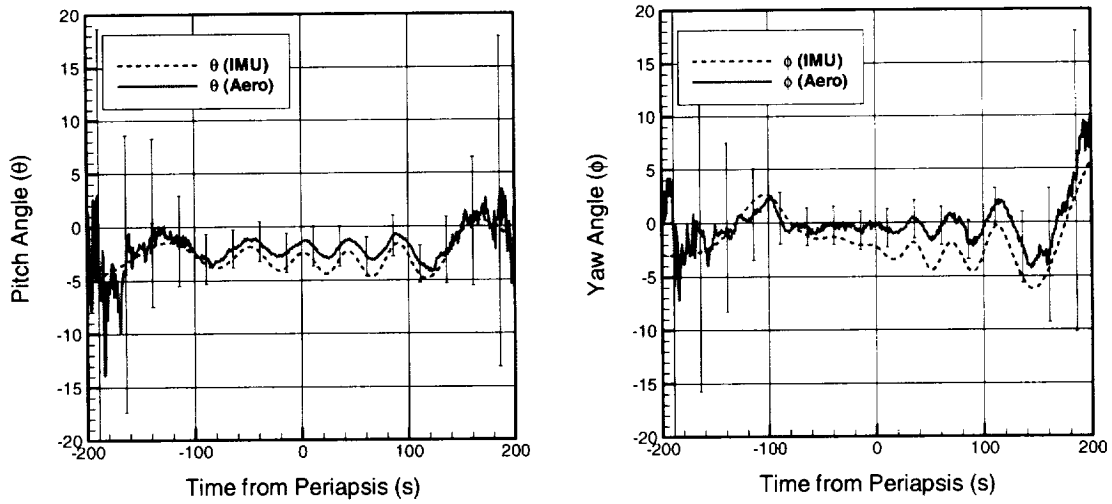


Figure 11. Spacecraft attitude comparison for aerobraking pass 170.

### Aerobraking Pass 112



### Aerobraking Pass 165

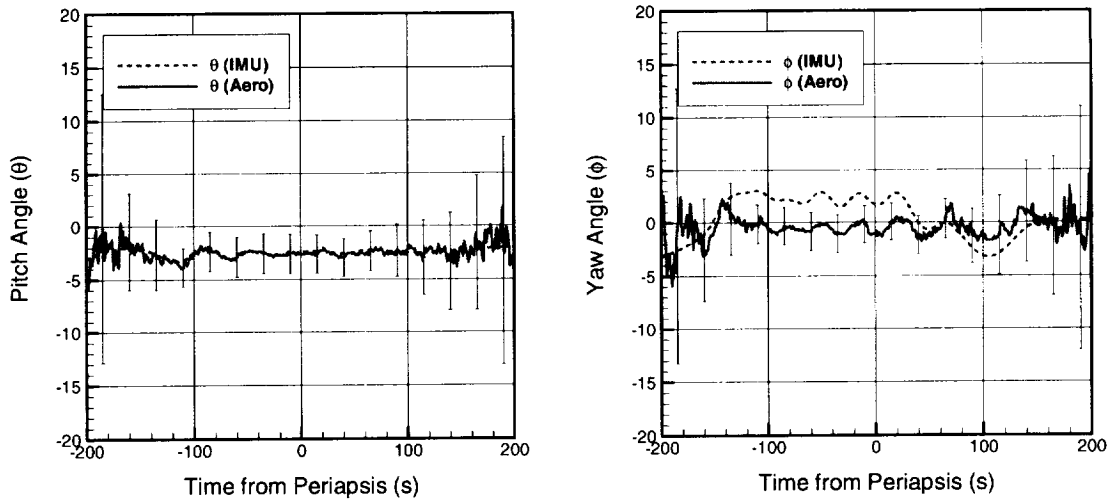


Figure 12. Spacecraft attitude comparisons for aerobraking passes 112 and 165.

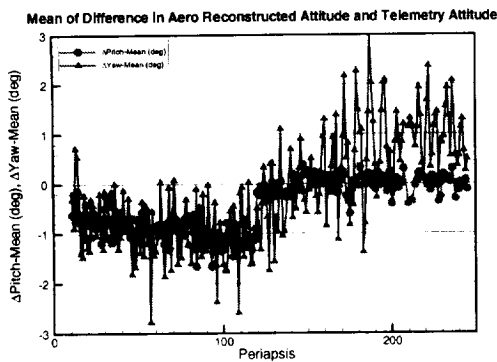


Figure 13. Variation of mean of differences in spacecraft attitude with aerobraking passes.

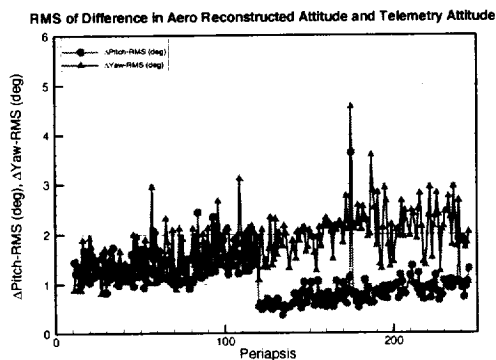


Figure 14. Variation of RMS of differences in spacecraft attitude with aerobraking passes.

### Conclusions

DSMC and free-molecular methods were used to provide aerothermodynamic predictions for the Mars Odyssey spacecraft. The predictions were used to create an aerodynamic database that was used for numerous trajectory simulations both prior to and during aerobraking operations and to reconstruct atmospheric density profiles during each pass. The aerodynamic database was also used together with data obtained from on-board accelerometers to reconstruct the spacecraft attitudes throughout each aerobraking pass. The reconstructed spacecraft attitudes are in good agreement with those determined by independent on-board inertial measurements for all aerobraking passes. The differences in the pitch attitudes are significantly less than the preflight uncertainties of  $\pm 2.9\%$ . The differences in the yaw attitudes suggest influence zonal winds. When the latitudinal gradients of density are small, i.e., when the atmosphere is quiescent, the differences in the yaw attitudes are significantly less than the preflight uncertainties. Small discrepancies in pitch attitude between the accelerometer-derived and IMU-derived attitude were observed based on early

aerobraking passes that were empirically corrected for later passes. However, these discrepancies were much less than the estimated uncertainties in the aerodynamic predictions and had negligible effect on other flight data analyses that used the aerodynamic database. The apparent evidence of zonal winds observed by comparing the yaw angles derived from accelerometers and independent inertial attitude measurements raises interesting possibilities for future missions to study the upper atmosphere of Mars in more detail.

### Acknowledgments

The authors would like to acknowledge Doug Gulick of then Lockheed-Martin Astronautics (currently with Ball Aerospace), for providing the computational geometry, and Jim Chapel of Lockheed-Martin Astronautics for providing information on the Mars Odyssey spacecraft instruments.

### References

- 1 Lyons, D. T., "Aerobraking Magellan: Plan Versus Reality," AAS Paper 94-118, Feb. 1994.
- 2 Lyons, D. T., Beerer, J. G., Esposito, P., Johnston, M. D., "Mars Global Surveyor: Aerobraking Mission Overview," *Journal of Spacecraft and Rockets*, Vol. 36, No. 3, May-June, 1999.
- 3 Smith, J. and Bell, J., "2001 Mars Odyssey Aerobraking," AIAA 2002-4532, Aug. 2002.
- 4 Wilmoth, R.G., LeBeau, G. J., and Carlson, A. B., "DSMC Grid Methodologies for Computing Low-Density, Hypersonic Flows About Reusable Launch Vehicle," AIAA Paper 96-1812, June 1996.
- 5 LeBeau, G. J. and Lumpkin III, F. E., "Application Highlights of the DSMC Analysis Code (DAC) Software for Simulating Rarefied Flows," *Computer Methods in Applied Mechanics and Engineering*, Vol. 191, Issues 6-7, 7 December 2001, Pages 595-609.
- 6 Bird, G. A., *Molecular Gas Dynamics and the Direct Simulation of Gas Flows*, Clarendon Press, Oxford, 1994.
- 7 Moss, J. N., Blanchard, R. C., Wilmoth, R. G. and Braun, R. D., "Mars Pathfinder Rarefied Aerodynamics: Computation and Measurements," AIAA 98-0298, January 1998.
- 8 Tartabini, P., Munk, M. and Powell, R., "The Development and Evaluation of an Operational Aerobraking Strategy for the Mars 2001 Odyssey Orbiter," AIAA 2002-4537, Aug. 2002.
- 9 Tolson, R., Escalera, P., Dwyer, A., Hanna, J., "Application of Accelerometer Data to Mars Odyssey Aerobraking and Atmospheric Modeling," AIAA 2002-4533, August 2002.